



# The genetic and phenotypic spectra of adult genetic leukoencephalopathies in a cohort of 309 patients

Chujun Wu,<sup>1,2,†</sup> Mengwen Wang,<sup>3,†</sup> Xingao Wang,<sup>1,2</sup> Wei Li,<sup>1,2</sup> Shaowu Li,<sup>1,2</sup>  
Bin Chen,<sup>1,2</sup> Songtao Niu,<sup>1,2</sup> Hongfei Tai,<sup>1,2</sup> Hua Pan<sup>1,2</sup> and Zaiqiang Zhang<sup>1,2</sup>

<sup>†</sup>These authors contributed equally to this work.

Genetic leukoencephalopathies (gLEs) are a highly heterogeneous group of rare genetic disorders. The spectrum of gLEs varies among patients of different ages. Distinct from the relatively more abundant studies of gLEs in children, only a few studies that explore the spectrum of adult gLEs have been published, and it should be noted that the majority of these excluded certain gLEs. Thus, to date, no large study has been designed and conducted to characterize the genetic and phenotypic spectra of gLEs in adult patients.

We recruited a consecutive series of 309 adult patients clinically suspected of gLEs from Beijing Tiantan Hospital between January 2014 and December 2021. Whole-exome sequencing, mitochondrial DNA sequencing and repeat analysis of *NOTCH2NLC*, *FMR1*, *DMPK* and *ZNF9* were performed for patients. We describe the genetic and phenotypic spectra of the set of patients with a genetically confirmed diagnosis and summarize their clinical and radiological characteristics.

A total of 201 patients (65%) were genetically diagnosed, while 108 patients (35%) remained undiagnosed. The most frequent diseases were leukoencephalopathies related to *NOTCH3* (25%), *NOTCH2NLC* (19%), *ABCD1* (9%), *CSF1R* (7%) and *HTRA1* (5%). Based on a previously proposed pathological classification, the gLEs in our cohort were divided into leukovasculopathies (35%), leuko-axonopathies (31%), myelin disorders (21%), microgliopathies (7%) and astrocytopathies (6%). Patients with *NOTCH3* mutations accounted for 70% of the leukovasculopathies, followed by *HTRA1* (13%) and *COL4A1/2* (9%). The leuko-axonopathies contained the richest variety of associated genes, of which *NOTCH2NLC* comprised 62%. Among myelin disorders, demyelinating leukoencephalopathies (61%)—mainly adrenoleukodystrophy and Krabbe disease—accounted for the majority, while hypomyelinating leukoencephalopathies (2%) were rare. *CSF1R* was the only mutated gene detected in microgliopathy patients. Leukoencephalopathy with vanishing white matter disease due to mutations in *EIF2B2-5* accounted for half of the astrocytopathies.

We characterized the genetic and phenotypic spectra of adult gLEs in a large Chinese cohort. The most frequently mutated genes were *NOTCH3*, *NOTCH2NLC*, *ABCD1*, *CSF1R* and *HTRA1*.

- 1 Department of Neurology, Beijing Tiantan Hospital, Capital Medical University, 100070 Beijing, China
- 2 China National Clinical Research Centre for Neurological Disease, Beijing Tiantan Hospital, Capital Medical University, 100070 Beijing, China
- 3 Department of Neurology and Institute of Neurology of First Affiliated Hospital, Institute of Neuroscience, and Fujian Key Laboratory of Molecular Neurology, Fujian Medical University, 350005 Fuzhou, China

Received June 14, 2022. Revised September 30, 2022. Accepted November 01, 2022. Advance access publication November 16, 2022

© The Author(s) 2022. Published by Oxford University Press on behalf of the Guarantors of Brain.

This is an Open Access article distributed under the terms of the Creative Commons Attribution-NonCommercial License (<https://creativecommons.org/licenses/by-nc/4.0/>), which permits non-commercial re-use, distribution, and reproduction in any medium, provided the original work is properly cited. For commercial re-use, please contact [journals.permissions@oup.com](mailto:journals.permissions@oup.com)

Correspondence to: Zaiqiang Zhang  
Department of Neurology, Beijing Tiantan Hospital  
Capital Medical University, No.119 South 4th Ring West Road  
Fengtai District, Beijing 100070, China  
E-mail: ttyy0142011@126.com

**Keywords:** genetic leukoencephalopathy; leukodystrophy; white matter lesion; genetic spectrum; pathological classification

## Introduction

Genetic leukoencephalopathies (gLEs) are a highly heterogeneous group of rare disorders that predominantly affect CNS white matter.<sup>1</sup> They can occur at any age. Affected individuals have a wide spectrum of clinical presentations, including cognitive impairment, psychiatric symptoms, developmental retardation, stroke, ataxia, pyramidal signs, movement disorders, seizures, peripheral neuropathy and extraneurological symptoms.<sup>2</sup> The imaging patterns can vary according to the disease and its time course.<sup>3</sup>

Several large-scale studies have been conducted to describe the genetic spectrum of gLEs in childhood.<sup>4–7</sup> Metachromatic leukodystrophy (MLD) is the most common diagnosis and accounts for 8.2–25.3% of childhood gLEs.<sup>4–6</sup> Other main causes include adrenoleukodystrophy (ALD), Krabbe disease, mitochondrial disease, vanishing white matter disease (VWMD), Pelizaeus–Merzbacher disease and mucopolysaccharidoses.<sup>4–7</sup> Adult patients present with an obviously distinct disease spectrum compared to children. In a European study, cerebral autosomal dominant arteriopathy with subcortical infarcts and leukoencephalopathy (CADASIL) was the most frequent diagnosis, comprising 33% of adult gLEs.<sup>8</sup>

Adult gLEs are considered rare and difficult to diagnose. Therefore, only a few studies on the spectrum of adult gLEs have been published to date.<sup>8–11</sup> The results vary among these studies because of different inclusion and exclusion criteria, diagnostic methods and populations. In a cohort of 154 patients, CADASIL, VWMD, ALD and COL4A1-related disorders were the most common diagnoses.<sup>8</sup> In another study excluding classical leukodystrophies, VWMD ranked first place in adult gLEs, followed by CADASIL and adult-onset leukoencephalopathy with axonal spheroids and pigmented glia (ALSP).<sup>9</sup> In recent years, the detection of an increasing number of novel genes has contributed to a constantly changing genetic spectrum for gLEs.<sup>12–16</sup> In 2019, GGC expansion in NOTCH2NLC was found associated with neuronal intranuclear inclusion disease (NIID), and this exceeded CADASIL as the most frequently diagnosed cause of adult gLEs in a recent Japanese cohort.<sup>10,16</sup>

The clinical heterogeneity of gLEs reflects the contribution of diverse cellular pathologies. Genetic leukoencephalopathies can be caused by defects in any white matter structural components, including myelin, astrocytes, microglia, axons and blood vessels.<sup>17</sup> Genetic leukoencephalopathies with similar cellular pathology can share common clinical and radiological manifestations; therefore, knowledge of which cell types are primarily involved can be helpful in understanding clinical manifestations.<sup>17–19</sup>

In the present study, we describe the genetic and phenotypic spectra of adult gLEs based on a large Chinese cohort and summarize the clinical and radiological characteristics of the various pathological types of gLEs.

## Materials and methods

### Patients

A consecutive series of 309 adult patients clinically suspected of gLEs were recruited from the Department of Neurology, Beijing Tiantan Hospital, between January 2014 and December 2021. The inclusion criteria for adult patients clinically suspected of gLEs in our study were: (i) the presence of a progressive neurological syndrome and white matter lesions of the cerebrum/spinal cord on MRI or CT scan; (ii) acquired causes, including cerebrovascular diseases secondary to non-genetic causes (such as atherosclerosis and cardioembolism), toxic injuries, infection, drug-induced changes, inflammation, and neoplastic diseases were excluded; and (iii) at least 16 years old at the time of referral to our centre.

Clinical and imaging data were collected at the first visit to our clinic and were reviewed by at least two senior neurologists and a neuroradiologist. Written informed consent was obtained from all participants, and this study was approved by the Ethics Committees of Beijing Tiantan Hospital (ID of the ethics approval: KY2020-105-02).

### Genetic testing

#### Whole-exome sequencing

Whole-exome sequencing (WES) was conducted for all 309 patients. Genomic DNA was extracted from peripheral blood. WES was performed based on All Exon Kits (V6; Agilent) and then sequenced using the Illumina HiSeq2000 platform. Sequences were aligned to hg19 using the Burrows–Wheeler Aligner.<sup>20</sup> Single nucleotide variants and small insertions/deletions (indels) were identified using the Genome Analysis Toolkit and annotated using ANNOVAR.<sup>21,22</sup> Copy number variants were analysed by ExomeDepth.<sup>23</sup> Variants were filtered using the following criteria: (i) hypothesized inheritance pattern coherent with family history; (ii) allele frequency lower than 1% among recessive disease-associated genes and 0.1% among dominant disease-associated genes in each of the following databases: 1000 Genomes Project, ExAC and gnomAD; (iii) predicted deleterious effect on protein function; and (iv) canonical variants putatively altering splice sites. Predicted deleterious effects were analysed using SIFT, PolyPhen-2 (<http://genetics.bwh.harvard.edu/pph2/>) and MutationTaster (<https://www.mutationtaster.org/>), and the effects of variants on splicing were analysed using SpliceAI (<https://spliceailookup.broadinstitute.org/>).

All samples underwent a two-step analysis: in the first step, variants in genes previously reported as associated with gLEs were considered (listed in [Supplementary Table 1](#)).<sup>24</sup> In the second step, all heterozygous variants with an allele frequency <0.01%—as well as homozygous and potentially compound heterozygous variants—were considered.

All variants were classified according to the standards of the American College of Medical Genetics criteria.<sup>25</sup> Cases were considered to have a genetically confirmed diagnosis if variants were classified as pathogenic or likely pathogenic. Cases with a variant of unknown significance but compatible segregation analysis and specific clinical and imaging findings highly suggestive of a given disease were also considered genetically diagnosed.

### Analysis of repeat expansions

Trinucleotide repeat expansions of *NOTCH2NLC* were screened in 41 patients suspected of NIID. These cases were clinically diagnosed based on characteristic clinical symptoms, imaging features (e.g. high-intensity signal in the corticomedullary junction on diffusion-weighted imaging of brain MRI) and pathological findings (e.g. eosinophilic hyaline intranuclear inclusions in the skin biopsy).<sup>26</sup> Repeat-primed polymerase chain reaction (RP-PCR) and fluorescence amplicon length analysis-PCR (AL-PCR) were used to assess the number of GGC repeats in the *NOTCH2NLC* gene as reported previously.<sup>27</sup> As the cases with *FMR1* premutation show the symptoms and intranuclear inclusions as NIID, we analysed the CGG repeat length of *FMR1* in these patients to screen fragile X-associated tremor/ataxia syndrome.<sup>26,28</sup>

Three cases with prominent myotonia and muscle weakness were suspected of myotonic dystrophy and were screened for repeat expansions of *DMPK* and *ZNF9*.<sup>29,30</sup>

### Mitochondrial DNA sequencing

Mitochondrial DNA sequencing was performed on 12 patients clinically suspected of having mitochondrial diseases.<sup>31,32</sup> These patients had multiple-system involvement (e.g. myopathy, peripheral neuropathy, optic neuropathy, sensorineural hearing loss, diabetes, cardiac abnormality, gastrointestinal, renal or hepatic involvement) and lesions involving the cortex, basal ganglia or brainstem on MRI or CT scan.

### Classification system

The pathological classification used in the present study was based on a previous report.<sup>17</sup> All genetic leukoencephalopathies were classified based on pathological changes and primary involvement of white matter components.<sup>17</sup> According to this classification system, genetic leukoencephalopathies can be classified into five groups, including: (i) myelin disorders, in which oligodendrocytes and myelin are primarily or predominantly affected; (ii) astrocytopathies owing to defects in astrocyte-specific gene products or in which astrocyte dysfunctions play a major pathogenetic role; (iii) leuko-axonopathies secondary to neuronal or axonal defects; (iv) microgliopathies owing to defects in microglia-specific gene products; and (v) leukovasculopathies owing to vascular pathology. Myelin disorders can be subdivided into hypomyelinating leukoencephalopathies, demyelinating leukoencephalopathies and leukoencephalopathies with myelin vacuolization.

### Data availability

The authors confirm that the data supporting the findings of this study are available within the article and its [Supplementary material](#).

## Results

A total of 201 (65%) of the 309 individuals suspected of gLEs were genetically diagnosed, while 108 patients (35%) remained

undiagnosed in our cohort. Among the 201 patients with a genetically confirmed diagnosis, 156 patients (50%) were diagnosed based on the WES data, 42 patients (14%) were diagnosed based on repeat analysis of *NOTCH2NLC* (13%) and *DMPK* (1%), while three patients (1%) were diagnosed based on mitochondrial DNA sequencing.

The most frequently mutated genes were *NOTCH3* (25%), *NOTCH2NLC* (19%), *ABCD1* (9%), *CSF1R* (7%) and *HTRA1* (5%) ([Fig. 1A](#)). Based on pathological classification, the gLEs of our cohort were divided into leukovasculopathies (35%), leuko-axonopathies (31%), myelin disorders (21%), microgliopathies (7%) and astrocytopathies (6%) ([Fig. 1B](#)). The most helpful and discriminating clinical and imaging features related to specific gLEs are summarized in [Tables 1 and 2](#) and [Supplementary Table 2](#).

### Leukovasculopathies

The genetic spectrum of leukovasculopathies included *NOTCH3* (70%), *HTRA1* (13%), *COL4A1/2* (9%), *APP* (4%), *TREX1* (3%) and *GLA* (1%).

### CADASIL

A total of 50 CADASIL patients were identified. The average age at onset was  $41.8 \pm 10.7$  (mean  $\pm$  SD) years. Cognitive impairment (72%), ischaemic cerebrovascular disease (56%), psychiatric symptoms (46%) and migraine (24%) were common symptoms. Intracranial haemorrhage was rare (10%). Neuroimaging data were available for 42 CADASIL patients. White matter involvement of the bilateral external capsules and anterior temporal lobes ([Fig. 2A](#)) was observed in 83% and 64% of the patients, respectively. Lacunar infarctions (79%) and microbleeds (57%) were also common imaging findings. Thirty-four mutations were identified in the *NOTCH3* gene, including nine novel mutations ([Supplementary Tables 3 and 4](#)).

### CADASIL2

Heterozygous *HTRA1* mutations are associated with cerebral autosomal dominant arteriopathy with subcortical infarcts and leukoencephalopathy 2 (CADASIL2).<sup>15</sup> Nine probands and two affected siblings carrying heterozygous *HTRA1* mutations were diagnosed with CADASIL2. Biallelic mutations in *HTRA1* were not found in our cohort. The average age at onset was  $41.1 \pm 2.7$  years. Common neurological symptoms included cognitive impairment (100%), psychiatric symptoms (82%), gait disturbance (73%) and ischaemic stroke (64%). Three patients had spondylosis deformans ([Fig. 2B and C](#)). Alopecia was noted in one patient. Neuroimaging data were available for nine patients: all had moderate-to-severe leukoencephalopathy with involvement of bilateral external capsules (100%) and anterior temporal lobes (22%). Lacunar infarctions were observed in all nine patients and microbleeds were observed in six patients. Nine missense mutations in *HTRA1* were identified, including six novel mutations ([Supplementary Table 5](#)).

### COL4A1/2-related disorders

Six patients presented with *COL4A1/2*-related disorders. The average age at onset was  $45.8 \pm 11.1$  years. Intracranial haemorrhage was found in 2 patients ([Fig. 2D](#)) and recurrent brainstem infarctions were found in one patient with pontine autosomal dominant microangiopathy and leukoencephalopathy (PADMAL, [Fig. 2E and F](#)). Two patients who were previously diagnosed with hereditary angiopathy with nephropathy, aneurysm and muscle cramps (HANAC) syndrome had muscle cramps. Intracranial aneurysm was detected in one of the patients with HANAC. Extraneurological symptoms

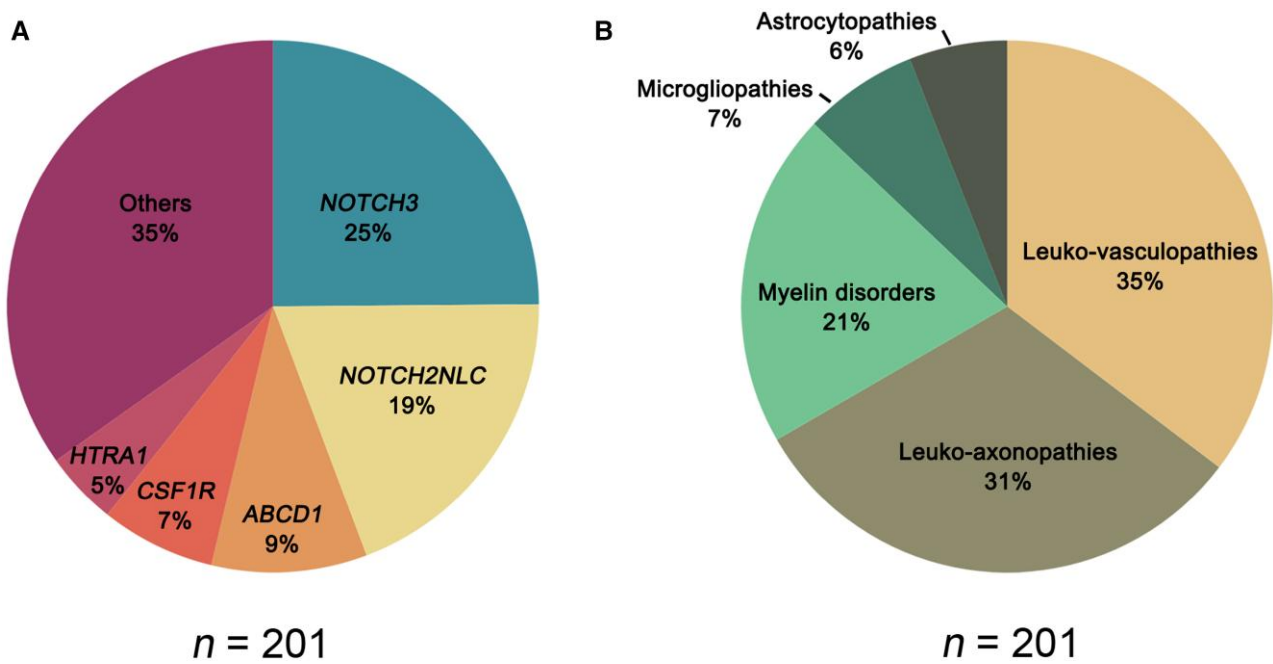


**Figure 1** Distribution of adult genetic leukoencephalopathies in our cohort. (A) Genetic spectrum of genetic leukoencephalopathies (n = 201). The five most frequently mutated genes are listed here. (B) Distribution of the five pathological subtypes of genetic leukoencephalopathies (n = 201).

affected the eyes (67%), kidneys (33%) and heart (33%). We identified a heterozygous c.\*34G>T mutation in the 3' untranslated region of the COL4A1 gene in the patient with PADMAL, three other mutations in the coding region of COL4A1 and two mutations in COL4A2 (Supplementary Table 6).

**Table 1** Clinical and imaging features of genetic cerebral small vessel disease in our cohort

Clinical features of genetic cerebral small vessel disease	
Ischaemic stroke or TIA	CADASIL, CADASIL2, PADMAL
Haemorrhagic stroke	COL4A1/2-related disorders, CADASIL
Migraine	CADASIL
Spondylosis deformans	CADASIL2
Paroxysmal muscle spasm	HANAC
Neuropathic pain	Fabry disease
Angiokeratoma	Fabry disease
Renal involvement	COL4A1/2-related disorders, Fabry disease, RVCL-S
Eye involvement	COL4A1/2-related disorders, RVCL-S
Imaging features of genetic cerebral small vessel disease	
Anterior temporal lobe signal abnormality	CADASIL, CADASIL2
External capsule signal abnormality	CADASIL, CADASIL2
Lacunar infarctions	CADASIL, CADASIL2
Cerebral microbleeds	CAA, COL4A1/2-related disorders, CADASIL, CADASIL2
Recurrent brainstem infarctions	PADMAL
Pseudotumor sign	RVCL-S

CAA = cerebral amyloid angiopathy; HANAC = hereditary angiopathy with nephropathy, aneurysms, and muscle cramps; PADMAL = pontine autosomal dominant microangiopathy and leukoencephalopathy; RVCL-S = autosomal dominant retinal vasculopathy with cerebral leukoencephalopathy and systemic manifestations; TIA = transient ischaemic attacks.

**Hereditary cerebral amyloid angiopathy**

Three probands from three different families had the same heterozygous mutation c.2059A>C (p.K687Q) in APP. All three patients developed cognitive impairment in their 40s. Multiple cortical and subcortical microbleeds were observed in two patients.

**Retinal vasculopathy with cerebral leukodystrophy and systemic manifestations**

Two patients had heterozygous TREX1 mutations: c.811\_812dupA (p.D272Rfs\*6) or c.748\_758del (p.T250Pfs\*8). Both patients presented with retinal vasculopathy and hemiplegia in adulthood. Renal failure was detected in one patient and seizures were detected in the other patient. Brain imaging of both patients showed enhanced lesions with a mass effect and surrounding oedema on MRI (Fig. 2G) and punctate calcifications beyond the lesion by CT scan (Fig. 2H).

**Fabry disease**

We identified a male patient with the GLA mutation c.672T>G (p.N224K). The patient presented with burning pain of the feet and reduced sweating in early life. He was referred to our hospital for recurrent ischaemic attacks at the age of 25. Angiokeratoma and proteinuria were detected.

**Myelin disorders**

The myelin disorder cases in our cohort could be subdivided into hypomyelinating leukoencephalopathies (2%), demyelinating leukoencephalopathies (61%) and leukoencephalopathies with myelin vacuolization (37%). The genetic causes of this group included GJC2, ABCD1, GALC, CYP27A1, GJB1, PAH, MMACHC, MTHFR, GCDH and LMNB1. The most common mutated gene was ABCD1 (46%).



**Table 2 Clinical and imaging features of hereditary non-vascular leukoencephalopathy in our cohort**

Clinical characteristics of hereditary non-vascular leukoencephalopathy	
Psychiatric symptoms	ALD, CblC disease, NIID, AARS2-L, ALSP, VWMD
Cognitive impairment	ALD, CblC disease, NIID, AARS2-L, ALSP, VWMD
Early prominent ataxia	CTX, Alexander's disease, Pol-III-related disorders, GHS, ALD, LBSL, ALSP, VWMD
Palatal myoclonus	Alexander's disease
Peripheral neuropathy	ALD, Krabbe disease, CTX, CMT-X, CblC disease, MTHFR deficiency, NIID, LBSL, mitochondrial disease, HSP
Autonomic symptoms	ADLD, NIID
Myopathy	DM1, LGMDR23, mitochondrial disease, AARS2-L, NIID
Rapid deterioration following head trauma	ALD, VWMD
Optic nerve atrophy	ALD, LBSL, AARS2-L, mitochondrial disease, VWMD, DM1
Cataract	CTX, DM1
Oligodontia	Pol-III-related disorders
Adrenocortical insufficiency	ALD
Premature ovarian failure	VWMD, AARS2-L
Hypogonadotrophic hypogonadism	GHS, Pol-III-related disorders
Tendon xanthoma	CTX
Imaging characteristics of hereditary non-vascular leukoencephalopathy	
Corpus callosum involvement	ALSP, VWMD, AARS2-L, HSP (SPG11, SPG15, SPG7), ADLD, NIID
Abnormal signal along pyramidal tract	Krabbe disease, Pol-III-related disorders
Spinal cord and brainstem involvement	Alexander's disease, LBSL
Cerebellar dentate nucleus	CTX, ALD
Cerebellar vermis	NIID
Middle cerebellar peduncles	NIID, LKPAT, ALD, LBSL, VWMD
Cystic degeneration	VWMD
Punctate calcification	ALSP, ALD
Contrast enhancement	ALD
Deep white matter diffusion dots	ALSP, AARS2-L, LBSL
High signals along the corticomedullary junction on DWI	NIID
Transient and reversible white matter lesions	CMT-X

AARS2-L = AARS2-related leukodystrophy; ADLD = adult-onset autosomal dominant leukodystrophy; CblC = methylmalonic aciduria and homocystinuria cblC type; CMT-X = X-linked Charcot-Marie-Tooth; CTX = cerebrotendinous xanthomatosis; DM1 = myotonic dystrophy type 1; DWI = diffusion weighted imaging; GHS = Gordon Holmes syndrome; HSP = hereditary spastic paraplegia; LBSL = leukoencephalopathy with brainstem and spinal cord involvement with elevated lactate; LGMDR23 = autosomal recessive limb-girdle muscular dystrophy-23; LKPAT = leukoencephalopathy with ataxia; MTHFR deficiency = methylenetetrahydrofolate reductase deficiency; SPG = spastic paraplegia.

## Hypomyelinating leukoencephalopathies

### Pelizaeus–Merzbacher-like disease

We identified novel compound heterozygous *GJC2* mutations in a female with Pelizaeus–Merzbacher-like disease (Supplementary Table 7). She had psychomotor retardation and nystagmus in early life and developed progressive spasticity and ataxia at the age of 20. A brain CT scan showed symmetric hypointensities in the periventricular white matter.

## Demyelinating leukoencephalopathies

### Adrenoleukodystrophy

A total of 19 male patients were identified (Supplementary Table 8). According to clinical and imaging manifestations, they were classified into childhood cerebral ALD (CCALD, 1/19), adolescent cerebral ALD (AdoCALD, 2/19), adult cerebral ALD (ACALD, 6/19), adrenomyeloneuropathy (AMN, 8/19) and spinocerebellar variant ALD (2/19). Seven patients (37%) had adrenocortical insufficiency. Nineteen mutations were found, including six novel mutations (Supplementary Table 8).

In nine patients with cerebral ALD, cognitive impairment (100%), psychiatric disorders (89%), pyramidal signs (78%), ataxia (56%), sphincter dysfunction (44%) and seizures (44%) were

common neurological symptoms. Three patients deteriorated after head trauma. Brain MRI was available for five patients. Three patients had white matter changes with occipitoparietal predominance and two had frontal predominance (Fig. 3A and B). Diffusion-weighted imaging (DWI) hyperintensities and Gd enhancement in the outer layer of lesions were observed in five and two patients, respectively (Fig. 3C). A CT scan showed punctate calcification in one patient (Fig. 3D).

All patients with AMN or spinocerebellar variants developed symptoms in adulthood. Spastic paraplegia (8/8) was the most frequent symptom in AMN, followed by sphincter dysfunction (6/8), peripheral neuropathy (3/8), deep sensory disturbance (2/8), ataxia (2/8) and impotence (1/8). Both patients diagnosed with spinocerebellar variants presented with cerebellar ataxia, dysarthria and pyramidal signs. Symmetrical T<sub>2</sub>-weighted hyperintensities in the cerebellar dentate nucleus were characteristic imaging findings of the spinocerebellar variant (Fig. 3E).

### Krabbe disease

Four patients were diagnosed with Krabbe disease (Supplementary Table 7). Three patients presented with spastic paraplegia/hemiplegia and another patient presented with progressive left upper limb wasting and weakness. Corticospinal tract hyperintensities

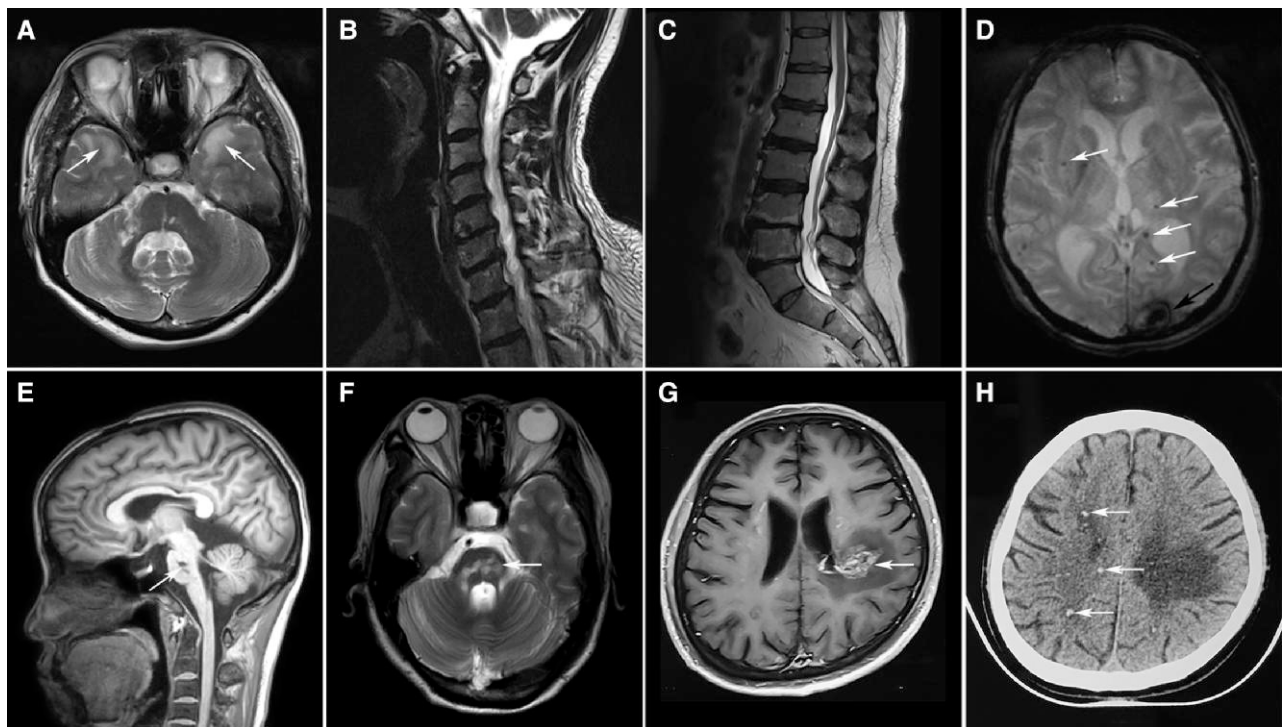


**Figure 2** Characteristic MRI features of genetic cerebral small vessel disease. (A) T<sub>2</sub> axial image showed hyperintensities of the anterior temporal lobes (arrows) in a 47-year-old patient with CADASIL. (B) Cervical MRI showed spondylosis deformans in a 57-year-old male patient carrying a heterozygous HTRA1 mutation. His affected brother suffered long-term low back pain and lumbar MRI showed spondylosis deformans (C). (D) Susceptibility-weighted image showed intracranial haemorrhage in the left occipital cortex (arrow) and multiple cerebral microbleedings (CMBs, arrows) in a 66-year-old patient with COL4A2-related disorders. (E and F) T<sub>1</sub> sagittal and T<sub>2</sub> axial images showed fused infarctions (arrows) in the pons in a 43-year-old patient with pontine autosomal dominant microangiopathy and leukoencephalopathy (PADMAL). (G) Post-contrast MRI of a 41-year-old patient with retinal vasculopathy with cerebral leukodystrophy and systemic manifestations (RVCL-S) showed an enhanced lesion with a mass effect and surrounding oedema (arrow) in the left parietal white matter. Punctate calcifications (arrows) were detected in the patient by the CT scan (H).

on T<sub>2</sub>-weighted images were observed in two patients presenting with spastic paraplegia/hemiplegia (Fig. 3F and G).

#### Cerebrotendinous xanthomatosis

Two patients with cerebrotendinous xanthomatosis (CTX) developed cerebellar ataxia in early life, followed by mental retardation, dysarthria, spastic paraplegia, peripheral neuropathy and cataracts (Supplementary Table 7). One of them had sensorineural deafness and chronic diarrhoea. Tendon xanthomata was found in the other patient. T<sub>2</sub>-weighted hyperintensities in the bilateral cerebellar dentate nucleus were found in both patients (Fig. 3H).

#### Leukoencephalopathies with myelin vacuolization

##### X-linked Charcot–Marie–Tooth

Three male patients carried hemizygous mutations in GJB1 (Supplementary Table 7). All of the patients presented with slowly progressive distal muscle weakness and atrophy. Sensorineural hearing loss was noted in one patient. Nerve conduction studies in all patients showed slow motor conduction velocities and low-amplitude compound muscle action potentials. Brain MRI in two patients showed transient and reversible white matter lesions with a predominance in the parietal region, which were hyperintensities on DWI and hypointensities on apparent diffusion coefficient imaging (Fig. 3I and J).

#### Disorders of amino acid and organic acid metabolism

Four male patients with phenylketonuria (PKU) developed mental retardation, light pigmentation of skin and a musty odour in early life (Supplementary Table 7). Their brain MRIs showed diffuse white matter lesions in parallel with the lateral ventricles (Fig. 3K).

Four patients with MMACHC mutations and two with MTHFR mutations shared some similar symptoms, including spastic paraplegia and peripheral neuropathy (Supplementary Table 7). However, patients with MMACHC mutations tended to present with cognitive impairment and psychiatric symptoms as their initial manifestations.

One male patient born to consanguineous parents carried homozygous mutations in GCDH (Supplementary Table 7). He presented with severe paroxysmal headache and mild cognitive impairment in his 20s. Diffuse white matter lesions were detected in bilateral periventricular areas and the centrum semiovale.

#### Adult-onset autosomal dominant leukodystrophy

We identified LMNB1 gene duplication in a male patient. He presented with spastic paraparesis, parkinsonism, dysarthria, chronic constipation and insomnia at the age of 59. Brain MRI showed extensive T<sub>2</sub>-weighted hyperintensities in the subcortical and deep white matter with relative sparing of the periventricular rim (Fig. 3L). Ventricular enlargement and thinning of the corpus callosum were also noted.

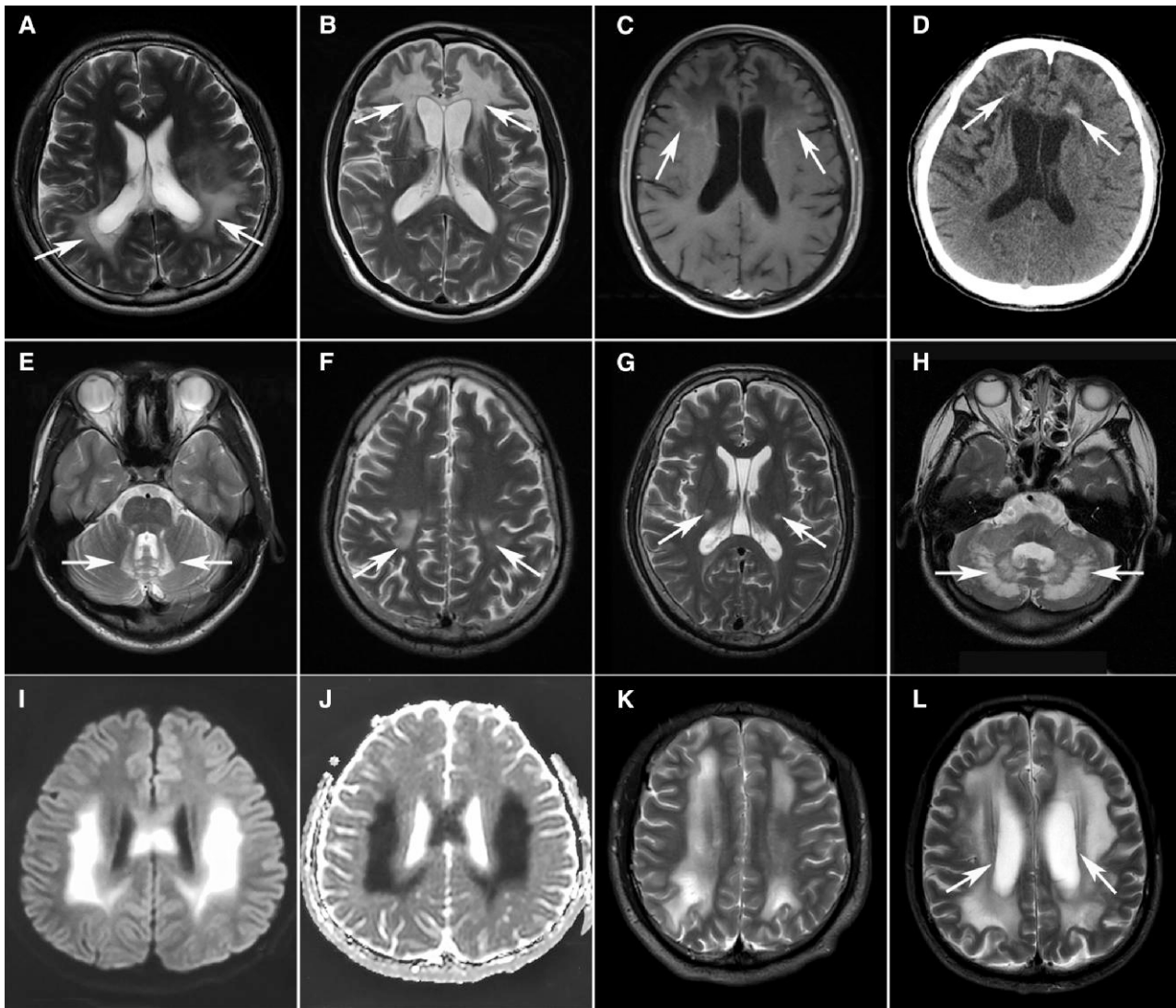


**Figure 3** Characteristic MRI features of myelin disorders. (A–E) Cerebral ALD with parieto-occipital (A, arrows) or frontal (B, arrows) predominance. Note the contrast enhancement (arrows) marginal to the demyelinated areas (C) and punctate calcification (arrows) in the lesions on CT scan (D). The spinocerebellar variant involved the bilateral cerebellar dentate nucleus (E, arrows). (F and G) Bilateral T<sub>2</sub> hyperintensity of corticospinal tracts from the motor cortex (F, arrows) along the posterior limb of the internal capsule (G, arrows) to the brainstem in a 46-year-old patient with Krabbe disease. (H) T<sub>2</sub>-weighted hyperintensities in the bilateral cerebellar dentate nucleus (arrows) in a 36-year-old female patient with cerebrotendinous xanthomatosis (CTX). (I and J) Hyperintensities on diffusion-weighted imaging (I) and hypointensities on apparent diffusion coefficient imaging (J) in the bilateral parietal regions in a 21-year-old male patient with X-linked Charcot–Marie–Tooth disease (CMT-X). (K) Diffuse white matter lesions in parallel with the lateral ventricles in a 23-year-old patient with phenylketonuria (PKU). (L) Extensive T<sub>2</sub>-weighted hyperintensities in the subcortical and deep white matters with relative sparing of the periventricular rim (arrows) in a 66-year-old patient with adult-onset autosomal dominant leukodystrophy (ADLD).

### Leuko-axonopathies

The genetic spectrum of leuko-axonopathies included *NOTCH2NLC*, *AARS2*, *DARS2*, Mt DNA, *SPG11*, *ZFYVE26*, *SPG7*, *POLR3A*, *RNF216*, *HEXB*, *IDS* and *DMPK*. The most frequently mutated gene was *NOTCH2NLC* (62%).

### Neuronal intranuclear inclusion disease

In our cohort, 39 patients were diagnosed with NIID (Supplementary Table 9). The number of GGC repeat expansions in *NOTCH2NLC* was between 87 and 159. Twenty-five (64%) patients were female. The mean age of onset was  $54.9 \pm 9.4$  years. Cognitive impairment (92%), autonomic dysfunction (79%), episodic neurological events (64%), tremor (54%), psychiatric symptoms (49%)

and headache (46%) were the most common symptoms. Episodic neurological events included disturbances of consciousness, encephalitic episodes, stroke-like episodes, epilepsy, paroxysmal headache, dizziness, nausea and vomiting.

Brain MRI was available for 35 patients. Dilated lateral ventricles (97%), high signals along the corticomedullary junction on DWI (Fig. 4A, 86%) and diffuse white matter lesions (80%) were the characteristic signs. T<sub>2</sub> hyperintensities in the cerebellar vermis (Fig. 4B) and middle peduncle were present in 40% and 20% of the patients, respectively.

### AARS2-related leukodystrophy

We identified four patients with biallelic mutations in *AARS2* (Supplementary Table 10). Three patients developed cognitive



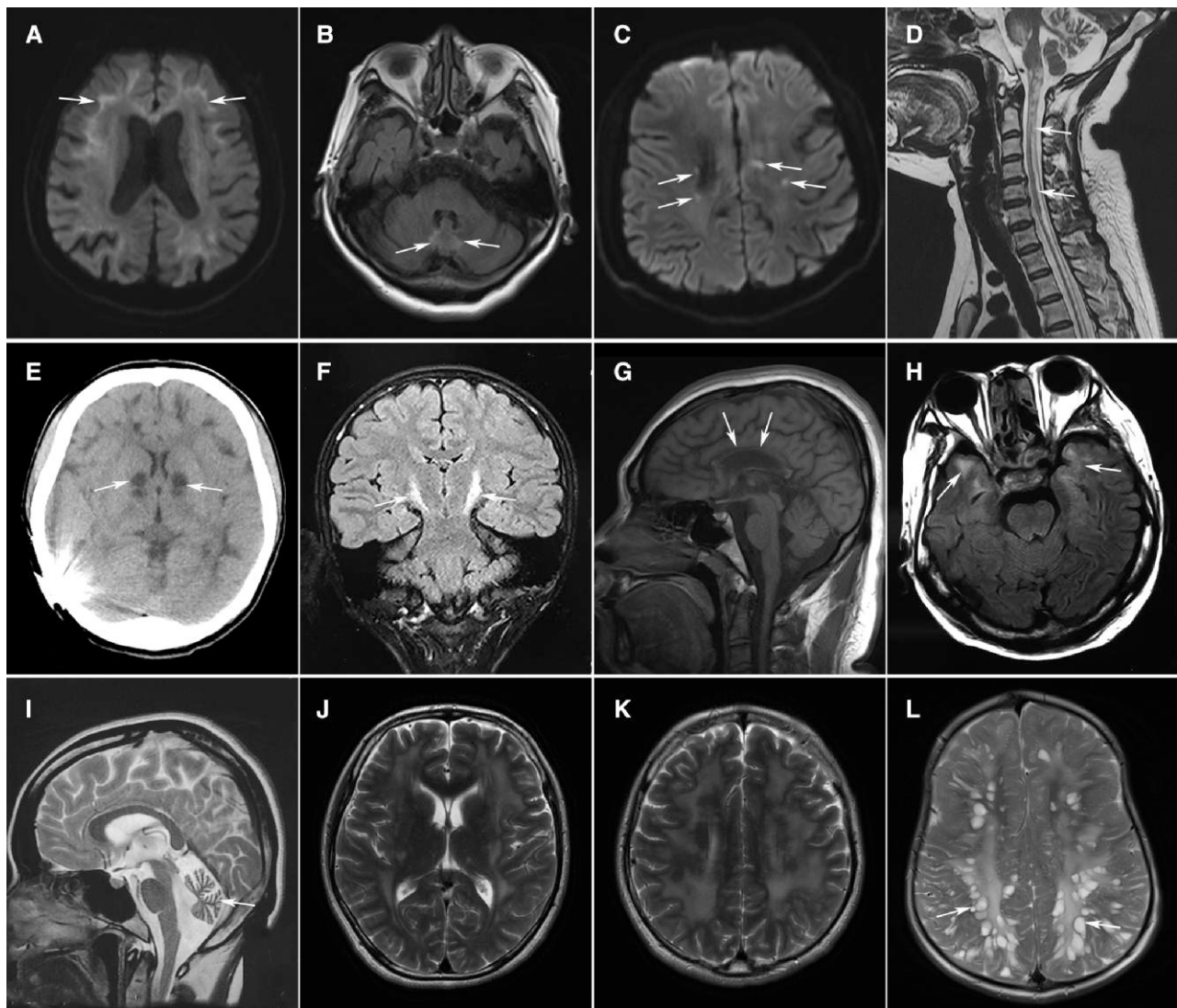


**Figure 4** Characteristic imaging features of leuko-axonopathies. (A and B) High signals on diffusion-weighted imaging (DWI) along the corticomedullary junction (A, arrows) and T<sub>2</sub>-weighted hyperintensities in the cerebellar vermis (B, arrows) in a 65-year-old female with NIID. (C) Punctate hyperintensity (arrows) within the white matter lesions on DWI in a 29-year-old male with AARS2-related leukoencephalopathy. (D) Long-tract involvement of the spinal cord (arrows) in a 36-year-old female with leukoencephalopathy with brainstem and spinal cord involvement and elevated cerebrospinal fluid lactate (LBSL). Severe cerebellar atrophy was also noted. (E) Abnormal signals of the basal ganglia (arrows) and diffuse white matter lesions on CT scan in a 19-year-old male patient with mitochondrial disease. (F) Hyperintensities along bilateral corticospinal tracts (arrows) on coronal FLAIR images in a male patient with Pol-III-related disorder. (G) Severe atrophy of the corpus callosum (arrows) in a 25-year-old female with spastic paraplegia-15 (SPG15). (H) Diffuse white matter lesions with the involvement of temporal lobes (arrows) in a patient with myotonic dystrophy type 1. (I) Marked cerebellar atrophy in a 26-year-old female with Sandhoff disease. (J and K) Extensive white matter lesions in a 27-year-old male with Gordon Holmes syndrome. (L) Enlarged perivascular spaces resembling bunches of grapes in a male patient with mucopolysaccharidosis type II.

impairment, psychiatric disorders and motor dysfunction in adulthood. Another male patient suffered delayed motor development in infancy and developed cognitive impairment and psychiatric symptoms at the age of 25. The only female patient had premature ovarian failure at the age of 35. All of the patients shared similar imaging findings, including periventricular white matter lesions, corpus callosum atrophy, mild ventricular enlargement and punctate DWI hyperintensities within white matter lesions (Fig. 4C).

#### Leukoencephalopathy with brainstem and spinal cord involvement and lactate elevation

We identified a patient with compound heterozygous mutations in DARS2 (Supplementary Table 10). The patient presented with delayed

motor development in infancy and was admitted to our hospital for slowly progressive ataxia and weakness in the lower limbs. Brain and spinal cord MRI showed T<sub>2</sub> hyperintensities in the periventricular white matter, medullary pyramids, medial lemniscus, dorsal columns and lateral corticospinal tracts of the spinal cord (Fig. 4D). Diffusion-weighted imaging revealed symmetric hyperintensities in the medullary pyramids, middle and inferior cerebellar peduncles, cerebellar dentate nucleus and cerebellar vermis. In the supratentorial area, punctate hyperintensities on DWI were distributed in periventricular white matter lesions (Supplementary Figure 1).

#### Mitochondrial DNA mutations

We identified three patients with mitochondrial DNA mutations (Supplementary Table 10). These patients presented with variable



combinations of cognitive decline, psychiatric symptoms, extrapyramidal symptoms, ataxia, ophthalmoplegia, sensorineural deafness, epilepsy, myopathy and peripheral neuropathy. Abnormal signals in the basal ganglia were observed in all three patients. Diffuse white matter lesions were found in one patient (Fig. 4E) and asymmetrical periventricular white matter lesions were found in the other two patients.

### Pol-III-related disorders

We identified two patients with compound heterozygous POLR3A mutations (Supplementary Table 10). They presented with progressive ataxia and spastic paraplegia since childhood. Oligodontia and intellectual disability were noted in one patient. Both had poor pubertal development. T<sub>2</sub> hyperintensities in pyramidal tracts were detected in both patients (Fig. 4F).

### Hereditary spastic paraplegia

We found white matter lesions in eight patients with hereditary spastic paraplegia (SPG), including five patients with SPG11, two with SPG15 and one with SPG7 (Supplementary Table 10). All of the patients except the one with SPG7 developed spastic paraplegia in adolescence. Periventricular white matter lesions accompanied by corpus callosum atrophy were the distinct imaging manifestations (Fig. 4G).

### Myotonic dystrophy type 1

Three male patients were diagnosed with myotonic dystrophy type 1 (Supplementary Table 10). All of them presented with myotonia, weakness and muscle wasting in early adulthood or adolescence. Mild cognitive impairment, sensorineural deafness, alopecia and cataracts were also common symptoms. Brain MRI showed diffuse white matter lesions with the involvement of temporal lobes in one patient (Fig. 4H). Patchy periventricular or subcortical white matter lesions were observed in the other two patients.

### Sandhoff disease, Gordon Holmes syndrome and mucopolysaccharidosis type II

We identified compound heterozygous HEXB mutations in a patient with Sandhoff disease (Supplementary Table 10). She presented with lower motor neuron syndrome at the age of 23. Brain MRI showed marked cerebellar atrophy (Fig. 4I).

Novel homozygous mutations in RNF216 were detected in a male patient diagnosed with Gordon Holmes syndrome (GHS; Supplementary Table 10). The patient had a history of hypogonadotropic hypogonadism and developed ataxia, dysarthria and cognitive impairment at the age of 26. Brain MRI revealed extensive white matter lesions and cerebellar atrophy (Fig. 4J and K).

We identified a novel hemizygous IDS mutation in a male patient with mucopolysaccharidosis type II (MPS II; Supplementary Table 10). He suffered recurrent upper respiratory tract infections in childhood and had abdominal protuberance, macrocephaly, skeletal deformities and amblyopia. Brain MRI showed enlarged perivascular spaces that were clustered, resembling bunches of grapes (Fig. 4L).

### Microgliopathies

#### Adult-onset leukoencephalopathy with axonal spheroids and pigmented glia

There were 14 patients diagnosed with ALSP (Supplementary Table 11). The average age of onset was 36.9 ± 9.1 years. Pyramidal

signs (86%), cognitive impairment (71%), ataxia (57%), psychiatric symptoms (43%) and parkinsonism (14%) were the common symptoms (Supplementary Table 11). Brain MRI data were available for eight patients and revealed periventricular white matter lesions (Fig. 5A), dilated lateral ventricles and thinning of the corpus callosum. Seven patients (88%) had characteristic punctate DWI hyperintensities within white matter lesions (Fig. 5B). All 11 mutations were located at exons 17–21, which encode the tyrosine kinase domain of the CSF1R protein (Supplementary Table 11).

### Astrocytopathies

The genetic spectrum of astrocytopathies comprised GFAP, EIF2B2-5, CLCN2 and LAMA2. VWMD caused by EIF2B2-5 mutations was the most common disease (50%).

### Vanishing white matter disease

We identified six patients with biallelic mutations in EIF2B2-5 (Supplementary Table 12). The age of onset ranged from infancy to 41 years. Cognitive impairment (100%), ataxia (83%), pyramidal signs (67%) and psychiatric symptoms (50%) were common neurological symptoms. Deterioration following head trauma was noted in two patients. Three of four female patients had premature ovarian failure. Diffuse white matter lesions with cystic degeneration were characteristic imaging findings (Fig. 5C and D). Thinning of the corpus callosum and T<sub>2</sub> hyperintensities in the middle cerebellar peduncles were also observed.

### Alexander's disease

Three patients with Alexander's disease were identified (Supplementary Table 12). The onset age of the patients ranged from infancy to adulthood. Progressive ataxia (3/3) and pyramidal signs (3/3) were the most frequent symptoms, followed by bulbar signs (2/3), bladder dysfunction (2/3), palatal myoclonus (1/3) and cognitive impairment (1/3). Brain MRI of all three patients showed prominent atrophy of the medulla and spinal cord (tadpole sign; Fig. 5E). Symmetric patchy or diffuse white matter lesions were located in the periventricular areas and centrum semiovale.

### Autosomal recessive limb-girdle muscular dystrophy-23

We identified two male patients with compound heterozygous mutations in LAMA2 (Supplementary Table 12). Both presented with seizures and one had progressive weakness of distal lower extremities. Diffuse white matter lesions with involvement of the anterior temporal lobes were detected in both patients (Fig. 5F).

### Leukoencephalopathy with ataxia

We identified a male patient with a novel homozygous mutation in CLCN2 (Supplementary Table 12). The patient suffered severe recurrent headache at the age of 41. A brain MRI showed T<sub>2</sub> hyperintensities in the middle cerebellar peduncles and posterior limbs of the internal capsule (Fig. 5G and H).

## Discussion

It has been established that gLEs represent a diverse group of diseases characterized by rarity, high heterogeneity and challenging diagnosis.<sup>33</sup> To the best of our knowledge, this is the largest cohort to date to explore the genetic and phenotypic spectra of adult gLEs. In our study, approximately two-thirds of genetic causes were

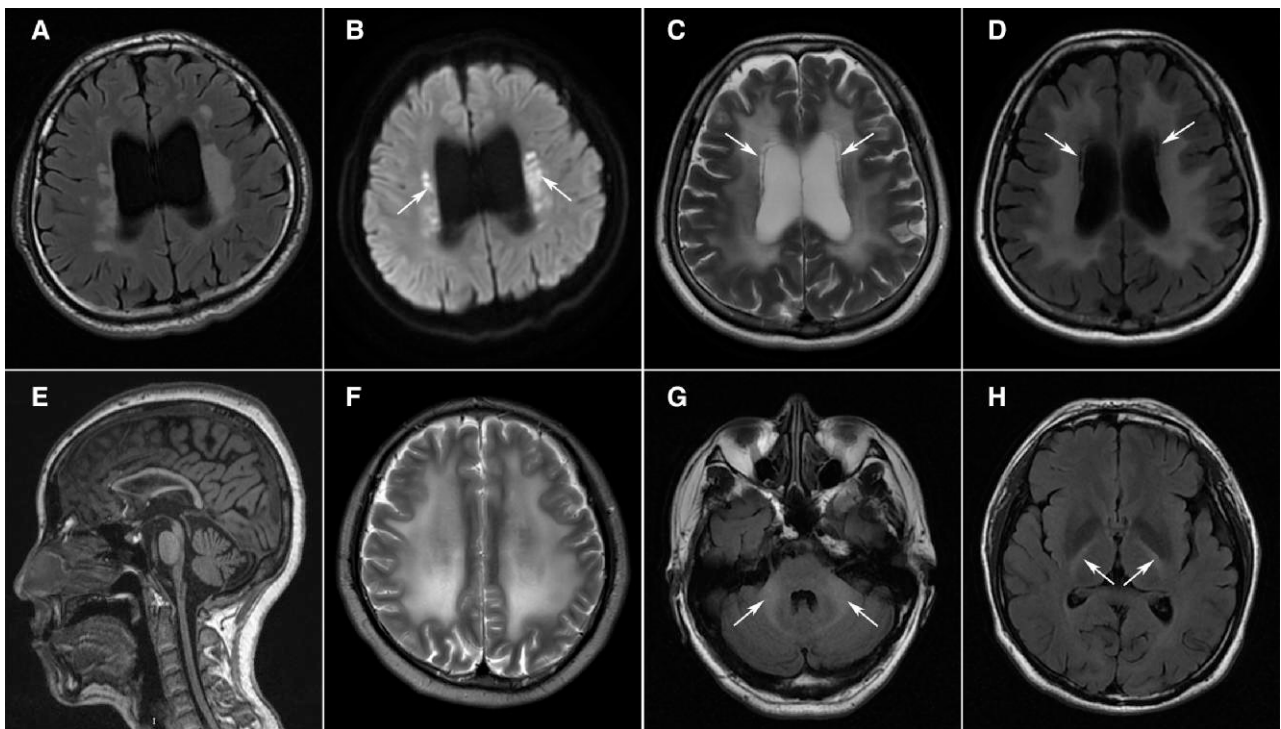


**Figure 5** Characteristic MRI features of microgliopathies and astrocytopathies. (A and B) Deep white matter lesions (A) and punctate DWI hyperintensities inside the white matter lesions (B, arrows) in a 28-year-old male with ALSP. (C and D) Diffuse white matter lesions with cystic degeneration (arrows) in a 29-year-old female with VWMD. (E) Severe brainstem and spinal cord atrophy in a 30-year-old female with Alexander's disease. (F) Diffuse white matter lesions in a 28-year-old male with LAMA2-related autosomal recessive limb-girdle muscular dystrophy-23 (LGMDR23). (G and H) The FLAIR images showed hyperintensities in the middle cerebellar peduncles (G, arrows) and posterior limbs of the internal capsules (H, arrows) in a 48-year-old male with CLC-2 chloride channel deficiency.

*NOTCH3*, *NOTCH2NLC*, *ABCD1*, *CSF1R* and *HTRA1*. *NOTCH3* and *NOTCH2NLC* far exceeded other genes and accounted for approximately half of the genetic causes. A recent Japanese study reported that *NOTCH2NLC* and *NOTCH3* were the most frequently mutated genes in adult gLEs and comprised 82% of all diagnosed patients.<sup>10</sup> Of note, GGC expansions in *NOTCH2NLC*, rather than *NOTCH3* mutations, were the most frequent cause in the Japanese study.<sup>10</sup> In European studies, *NOTCH3* and *EIF2B* mutations were the most common genetic causes of adult gLEs, accounting for 33% and 13% of diagnosed patients, respectively.<sup>8,9</sup> *ABCD1* and *CSF1R* mutations were also frequently detected in adult gLEs, while *HTRA1* mutations were rarely reported in previous cohort studies.<sup>8–10,34</sup>

According to the pathological classification proposed by van der Knaap and Bugiani,<sup>17</sup> leukovasculopathies in our cohort represent the largest proportion, followed by leuko-axonopathies, myelin disorders, microgliopathies and lastly astrocytopathies. Note that some disorders that are not considered primary genetic leukoencephalopathies but which are considered neurogenetic disorders with white matter abnormalities (e.g. X-linked Charcot-Marie-Tooth, CMT-X) were included in the present study. CMT-X is caused by mutations in *GJB1* coding for connexin-32 (Cx32).<sup>35</sup> Cx32 is a gap-junction channel-forming protein expressed in Schwann cells and oligodendrocytes, the myelinating glia of the peripheral and CNS, respectively.<sup>36</sup> Although CMT-X has been described as a peripheral neuropathy, CNS manifestations (e.g. acute episodic neurological dysfunction) have been reported in CMT-X.<sup>36</sup> Transient and reversible white matter lesions in bilateral deep white matter (as well as the corpus callosum) have been reported as characteristic imaging

features of CMT-X patients with episodic neurological dysfunction.<sup>37</sup> The CNS manifestations in CMT-X may be associated with loss of oligodendrocyte–oligodendrocyte and oligodendrocyte–astrocyte junctional coupling mediated by Cx32, while oligodendrocyte–oligodendrocyte coupling is likely to be the more important for the transient CNS dysfunction.<sup>38</sup> Accordingly, CMT-X is recognized as a genetic leukoencephalopathy and is classified among myelin disorders owing to the primary involvement of oligodendrocytes.<sup>1,17</sup>

The leukovasculopathies were the largest part of our gLE cohort. CADASIL due to *NOTCH3* mutations was the most frequent diagnosis and accounted for 70% of the leukovasculopathies and 25% of the patients with a genetically confirmed diagnosis. This proportion is slightly lower than reported in previous studies, in which CADASIL comprised 33–39% of all diagnosed gLE patients.<sup>8,10</sup> Although *HTRA1* mutations were rarely detected in previous cohort studies, they were the second most frequent genetic cause of leukovasculopathies in our cohort.<sup>8–10,34,39</sup> Interestingly, all the patients with *HTRA1*-related cerebral small vessel disease (CSVD) carried a heterozygous mutation, and no biallelic mutations in *HTRA1* were identified in our study, indicating that among Chinese patients heterozygous *HTRA1*-related CADASIL2 is more frequent than cerebral autosomal recessive arteriopathy with subcortical infarcts and leukoencephalopathy (CARASIL). *COL4A1/2*-related disorders were another common leukovasculopathy in our cohort; these were previously reported to constitute 7% of all diagnosed gLE patients in a European study.<sup>8</sup> In our patients, early-onset cognitive impairment and stroke, combined with lacunar infarctions and

microbleeds on MRI, are common characteristics of leukovascularopathies except for retinal vasculopathy with cerebral leukodystrophy and systemic manifestations (RVCL-S), which invariably mimics tumours.<sup>40</sup> Moreover, intracranial haemorrhage and multiple microbleeds are suggestive of COL4A1/2-related disorders or cerebral amyloid angiopathy.<sup>41</sup> Systematic involvement, including the eyes, kidney, skin and heart, is prominent in COL4A1/2-related disorders, Fabry disease and RVCL-S.<sup>41</sup> Spondylosis deformans is a distinct extraneurological symptom of HTRA1-related CSVD, with a frequency of 100% in CARASIL and 60% in CADASIL.<sup>42</sup>

The leuko-axonopathies constituted a variety of diseases, with NIID being the most frequent of these disorders. Given that CGG repeat expansions in *NOTCH2NLC* were only reported to be associated with NIID in 2019, to date, few studies have been conducted to explore the proportion of NIID among adult gLEs.<sup>10,16</sup> In agreement with a Japanese study,<sup>10</sup> our study found that NIID is a common genetic cause of adult gLEs in East Asia. Notably, a recent study screened *NOTCH2NLC* expansion in a European cohort of adult-onset leukoencephalopathy and did not identify any patients with GGC repeat expansion in *NOTCH2NLC*.<sup>43</sup> In the future, more studies are needed to profile the incidence of NIID in different populations. The phenotype of NIID is variable, while the imaging appearance is specific.<sup>26,44</sup> High-intensity signals in the corticomedullary junction on DWI were reported in 95.9% of NIID cases in a previous study.<sup>26</sup>

SPG11 mutations, which are the most common cause of complex hereditary spastic paraplegia,<sup>45</sup> were the second genetic cause of leuko-axonopathies in our cohort. In a previous study, two patients carrying SPG11 mutations were identified in 97 patients genetically diagnosed with gLEs, which is consistent with our results (5/201).<sup>8</sup> White matter abnormalities and corpus callosum thinning on MRI are the imaging features of SPG11.<sup>45</sup> AARS2 was another frequent genetic cause of leuko-axonopathies in our study but was rarely identified in previous cohorts.<sup>9,10,34,39</sup> For AARS2 mutation-related leukodystrophy, premature ovarian failure and punctate hyperintensities on DWI are the characteristic clinical and imaging signs.<sup>46</sup> Previous studies have also reported punctate hyperintensities on DWI for patients with leukoencephalopathy with brainstem and spinal cord involvement and elevated cerebrospinal fluid lactate (LBSL) or ALSP.<sup>46–48</sup> In our experience, the punctate diffusion restriction changes in the periventricular white matter appear similar among LBSL, ALSP and AARS2-related leukodystrophy (Supplementary Figure 2). It is difficult to distinguish these three diseases based solely on punctate diffusion restriction in the periventricular white matter. However, symmetric T<sub>2</sub>-weighted and DWI hyperintensities in the brainstem and cerebellum—which are distinctive imaging sign for patients with LBSL but rare in patients with ALSP or AARS2-related leukodystrophy—can be used to informatively distinguish LBSL from AARS2-related leukodystrophy and from ALSP.<sup>46–49</sup>

In myelin disorders, demyelinating leukodystrophies, including ALD and Krabbe disease, constitute the majority, while hypomyelinating leukodystrophies are rare. Note that MLD is the most common type of childhood leukoencephalopathy but was not found in the patients comprising our cohort.<sup>4–6</sup> ALD comprised 3.6–9.2% of childhood gLEs and 11.3% of adult gLEs in previous studies.<sup>4–8</sup> Although ALD is a frequent diagnosis in both child and adult patients with gLEs, the clinical phenotypes are different between the two groups.<sup>50</sup> Child patients frequently present with cerebral ALD and progress rapidly, while most adult patients present with adrenomyeloneuropathy (AMN) and progress slowly.<sup>50,51</sup> In our cohort, we found that AMN was the most common subtype and accounted for 42% of ALD cases. Approximately one-third of ALD patients presented with adult cerebral ALD in our cohort, suggesting that this

subtype is not rare in adult patients with ALD. Patients with cerebral ALD could deteriorate rapidly after head trauma,<sup>52,53</sup> as observed in our cohort: three cerebral ALD patients had a rapid deterioration and progression of neuroinflammation following head trauma. The spinocerebellar variant is a rare phenotype and accounts for 1–2% of ALD.<sup>54</sup> The actual proportion of spinocerebellar variants may be higher in Asia: we found that it was 10.5% in our cohort and was previously reported as 8.4% in a Japanese study.<sup>55</sup>

Microglia comprise a set of neurological phenotypes linked to mutations in *CSF1R*, *DAP12* and *TYROBP/TREM2*, *USP18*, *IRF8* and *NRROS*.<sup>56</sup> In our study, *CSF1R* was the only mutated gene detected in microgliopathy patients and comprised 7% of the genetically diagnosed patients. In a European cohort of 48 patients, *CSF1R* mutations accounted for 10% of idiopathic adult-onset leukodystrophies.<sup>57</sup> Nevertheless, the proportion of *CSF1R*-related disorders was lower in the other European study, accounting for 2% of adult gLEs.<sup>8</sup> ALSP is characterized by dementia, psychiatric changes and motor decline.<sup>58</sup> The MRI appearance is consistent among patients, including deep white matter lesions, enlargement of lateral ventricles, atrophy of the corpus callosum, punctate hyperintensities on DWI and calcifications.<sup>58</sup>

Although the astrocytopathies were the rarest group in our study, VWMD in the astrocytopathies is known as one of the most common gLEs in both children and adult patients.<sup>6,8,9</sup> The proportion of VWMD in gLEs ranged from 2% to 13% in paediatric studies<sup>4–7</sup> and reached 13% in a European study on adult gLEs.<sup>8</sup> In another European study excluding classical leukodystrophies, VWMD was the most frequent diagnosis in adult patients with gLEs and comprised 19% of diagnosed patients.<sup>9</sup> In our cohort, the frequency of VWMD (3%) was lower than that of previous European studies but similar to the findings of a Japanese study (1 patient with VWMD among 28 patients genetically diagnosed with gLE).<sup>10</sup> In clinical practice, typical cystic degeneration of the white matter and premature ovarian failure easily distinguish VWMD from other genetic leukoencephalopathies.<sup>59</sup>

In conclusion, we here described the genetic and phenotypic spectra of adult gLEs in a large Chinese cohort. In our cohort, *NOTCH3*, *NOTCH2NLC*, *ABCD1*, *CSF1R* and *HTRA1* were the most frequently mutated genes. It is worth noting that the GGC expansion in *NOTCH2NLC*, which might have been underestimated in previous studies, is a common genetic cause of adult gLEs in China. Our study should be beneficial for advancing clinical practice, genetic counselling and disease classification for adults with gLEs.

## Funding

No funding was received towards this work.

## Competing interests

The authors report no competing interests.

## Supplementary material

Supplementary material is available at *Brain* online.

## References

1. Vanderver A, Prust M, Tonduti D, et al. Case definition and classification of leukodystrophies and leukoencephalopathies. *Mol Genet Metab*. 2015;114:494–500.



2. Köhler W, Curiel J, Vanderver A. Adulthood leukodystrophies. *Nat Rev Neurol*. 2018;14:94-105.
3. Schiffmann R, van der Knaap MS. Invited article: An MRI-based approach to the diagnosis of white matter disorders. *Neurology*. 2009;72:750-759.
4. Bonkowsky JL, Nelson C, Kingston JL, Filloux FM, Mundorff MB, Srivastava R. The burden of inherited leukodystrophies in children. *Neurology*. 2010;75:718-725.
5. Stellitano LA, Winstone AM, van der Knaap MS, Verity CM. Leukodystrophies and genetic leukoencephalopathies in childhood: A national epidemiological study. *Dev Med Child Neurol*. 2016;58:680-689.
6. Alfadhel M, Almuqbil M, Al Mutairi F, et al. The leukodystrophy spectrum in Saudi Arabia: Epidemiological, clinical, radiological, and genetic data. *Front Pediatr*. 2021;9:633385.
7. Knuutinen OA, Oikarainen JH, Suo-Palosaari MH, et al. Epidemiological, clinical, and genetic characteristics of paediatric genetic white matter disorders in Northern Finland. *Dev Med Child Neurol*. 2021;63:1066-1074.
8. Ayriagnac X, Carra-Dalliere C, Menjot de Champfleury N, et al. Adult-onset genetic leukoencephalopathies: A MRI pattern-based approach in a comprehensive study of 154 patients. *Brain*. 2015;138:284-292.
9. Lynch DS, Rodrigues Brandão de Paiva A, Zhang WJ, et al. Clinical and genetic characterization of leukoencephalopathies in adults. *Brain*. 2017;140:1204-1211.
10. Okubo M, Doi H, Fukai R, et al. GGC Repeat expansion of NOTCH2NLC in adult patients with leukoencephalopathy. *Ann Neurol*. 2019;86:962-968.
11. Kunii M, Doi H, Ishii Y, et al. Genetic analysis of adult leukoencephalopathy patients using a custom-designed gene panel. *Clin Genet*. 2018;94:232-238.
12. Depienne C, Bugiani M, Dupuits C, et al. Brain white matter oedema due to CLC-2 chloride channel deficiency: An observational analytical study. *Lancet Neurol*. 2013;12:659-668.
13. Margolin DH, Kousi M, Chan YM, et al. Ataxia, dementia, and hypogonadotropism caused by disordered ubiquitination. *N Engl J Med*. 2013;368:1992-2003.
14. Dallabona C, Diodato D, Kevelam SH, et al. Novel (ovario) leukodystrophy related to AARS2 mutations. *Neurology*. 2014;82:2063-2071.
15. Verdura E, Hervé D, Scharrer E, et al. Heterozygous HTRA1 mutations are associated with autosomal dominant cerebral small vessel disease. *Brain*. 2015;138:2347-2358.
16. Sone J, Mitsuhashi S, Fujita A, et al. Long-read sequencing identifies GGC repeat expansions in NOTCH2NLC associated with neuronal intranuclear inclusion disease. *Nat Genet*. 2019;51:1215-1221.
17. van der Knaap MS, Bugiani M. Leukodystrophies: A proposed classification system based on pathological changes and pathogenetic mechanisms. *Acta Neuropathol*. 2017;134:351-382.
18. Yamamoto Y, Craggs L, Baumann M, Kalimo H, Kalaria RN. Review: Molecular genetics and pathology of hereditary small vessel diseases of the brain. *Neuropathol Appl Neurobiol*. 2011;37:94-113.
19. Berdowski WM, Sanderson LE, van Ham TJ. The multicellular interplay of microglia in health and disease: Lessons from leukodystrophy. *Dis Model Mech*. 2021;14:dmm048925.
20. Li H. Toward better understanding of artifacts in variant calling from high-coverage samples. *Bioinformatics*. 2014;30:2843-2851.
21. McKenna A, Hanna M, Banks E, et al. The genome analysis toolkit: A MapReduce framework for analyzing next-generation DNA sequencing data. *Genome Res*. 2010;20:1297-1303.
22. Wang K, Li M, Hakonarson H. ANNOVAR: Functional annotation of genetic variants from high-throughput sequencing data. *Nucleic Acids Res*. 2010;38:e164.
23. Plagnol V, Curtis J, Epstein M, et al. A robust model for read count data in exome sequencing experiments and implications for copy number variant calling. *Bioinformatics*. 2012;28:2747-2754.
24. Shukla A, Kaur P, Narayanan DL, do Rosario MC, Kadavigere R, Girisha KM. Genetic disorders with central nervous system white matter abnormalities: An update. *Clin Genet*. 2021;99:119-132.
25. Richards S, Aziz N, Bale S, et al. Standards and guidelines for the interpretation of sequence variants: A joint consensus recommendation of the American College of Medical Genetics and Genomics and the Association for Molecular Pathology. *Genet Med*. 2015; 17:405-424.
26. Sone J, Mori K, Inagaki T, et al. Clinicopathological features of adult-onset neuronal intranuclear inclusion disease. *Brain*. 2016;139:3170-3186.
27. Deng J, Gu M, Miao Y, et al. Long-read sequencing identified repeat expansions in the 5'UTR of the NOTCH2NLC gene from Chinese patients with neuronal intranuclear inclusion disease. *J Med Genet*. 2019;56:758-764.
28. Lyon E, Laver T, Yu P, et al. A simple, high-throughput assay for Fragile X expanded alleles using triple repeat primed PCR and capillary electrophoresis. *J Mol Diagn*. 2010;12:505-511.
29. Butterfield RJ, Imburgia C, Mayne K, et al. High throughput screening for expanded CTG repeats in myotonic dystrophy type 1 using melt curve analysis. *Mol Genet Genomic Med*. 2021;9:e1619.
30. Catali C, Morgante A, Iraci R, Rinaldi F, Botta A, Novelli G. Validation of sensitivity and specificity of tetraplet-primed PCR (TP-PCR) in the molecular diagnosis of myotonic dystrophy type 2 (DM2). *J Mol Diagn*. 2010;12:601-606.
31. Fang F, Liu Z, Fang H, et al. The clinical and genetic characteristics in children with mitochondrial disease in China. *Sci China Life Sci*. 2017;60:746-757.
32. Ng YS, Bindoff LA, Gorman GS, et al. Mitochondrial disease in adults: Recent advances and future promise. *Lancet Neurol*. 2021;20:573-584.
33. van der Knaap MS, Schiffmann R, Mochel F, Wolf NI. Diagnosis, prognosis, and treatment of leukodystrophies. *Lancet Neurol*. 2019;18:962-972.
34. Xie JJ, Ni W, Wei Q, et al. New clinical characteristics and novel pathogenic variants of patients with hereditary leukodystrophies. *CNS Neurosci Ther*. 2020;26:567-575.
35. Kleopa KA, Scherer SS. Molecular genetics of X-linked Charcot-Marie-Tooth disease. *Neuromolecular Med*. 2006;8:107-122.
36. Abrams CK, Freidin M. GJB1-associated X-linked Charcot-Marie-Tooth disease, a disorder affecting the central and peripheral nervous systems. *Cell Tissue Res*. 2015;360:659-673.
37. Tian D, Zhao Y, Zhu R, Li Q, Liu X. Systematic review of CMTX1 patients with episodic neurological dysfunction. *Ann Clin Transl Neurol*. 2021;8:213-223.
38. Abrams CK, Goman M, Wong S, et al. Loss of coupling distinguishes GJB1 mutations associated with CNS manifestations of CMT1X from those without CNS manifestations. *Sci Rep*. 2017;7:40166.
39. Vanderver A, Simons C, Helman G, et al. Whole exome sequencing in patients with white matter abnormalities. *Ann Neurol*. 2016;79:1031-1037.
40. Stam AH, Kothari PH, Shaikh A, et al. Retinal vasculopathy with cerebral leukoencephalopathy and systemic manifestations. *Brain*. 2016;139:2909-2922.
41. Sondergaard CB, Nielsen JE, Hansen CK, Christensen H. Hereditary cerebral small vessel disease and stroke. *Clin Neurol Neurosurg*. 2017;155:45-57.

42. Uemura M, Nozaki H, Kato T, et al. HTRA1-related cerebral small vessel disease: A review of the literature. *Front Neurol.* 2020;11:545.
43. Yau WY, Sullivan R, Chen Z, et al. GGC repeat expansion in NOTCH2NLC is rare in European leukoencephalopathy. *Ann Neurol.* 2020;88:641-642.
44. Fan Y, Xu Y, Shi C. NOTCH2NLC-related disorders: The widening spectrum and genotype-phenotype correlation. *J Med Genet.* 2022;59:1-9.
45. Kara E, Tucci A, Manzoni C, et al. Genetic and phenotypic characterization of complex hereditary spastic paraplegia. *Brain.* 2016;139:1904-1918.
46. Lakshmanan R, Adams ME, Lynch DS, et al. Redefining the phenotype of ALSP and AARS2 mutation-related leukodystrophy. *Neurol Genet.* 2017;3:e135.
47. Yelam A, Nagarajan E, Chuquilin M, Govindarajan R. Leukoencephalopathy with brain stem and spinal cord involvement and lactate elevation: A novel mutation in the DARS2 gene. *BMJ Case Rep.* 2019;12:bcr-2018-227755.
48. Werner R, Daum E, Felber S, Wöhrle JC. Leukoencephalopathy with brain stem and spinal cord involvement and not always lactate elevation. *Clin Neuroradiol.* 2018;28:451-453.
49. Kassem H, Wafaie A, Abdelfattah S, Farid T. Leukoencephalopathy with brainstem and spinal cord involvement and lactate elevation (LBSL): Assessment of the involved white matter tracts by MRI. *Eur J Radiol.* 2014;83:191-196.
50. Mao C, Li J, Huang X, et al. Typical and atypical phenotype and neuroimaging of X-linked adrenoleukodystrophy in a Chinese cohort. *Neurolo Sci.* 2022;43:3255-3263.
51. Engelen M, Kemp S, de Visser M, et al. X-linked adrenoleukodystrophy (X-ALD): Clinical presentation and guidelines for diagnosis, follow-up and management. *Orphanet J Rare Dis.* 2012;7:51.
52. Raymond GV, Seidman R, Monteith TS, et al. Head trauma can initiate the onset of adreno-leukodystrophy. *J Neurol Sci.* 2010;290:70-74.
53. Bouquet F, Dehais C, Sanson M, Lubetzki C, Louapre C. Dramatic worsening of adult-onset X-linked adrenoleukodystrophy after head trauma. *Neurology.* 2015;85:1991-1993.
54. Kemp S, Pujol A, Waterham HR, et al. ABCD1 mutations and the X-linked adrenoleukodystrophy mutation database: Role in diagnosis and clinical correlations. *Hum Mutat.* 2001;18:499-515.
55. Suzuki Y, Takemoto Y, Shimozaawa N, et al. Natural history of X-linked adrenoleukodystrophy in Japan. *Brain Dev.* 2005;27:353-357.
56. Smith C, McColl BW, Patir A, et al. Biallelic mutations in NRROS cause an early onset lethal microgliopathy. *Acta Neuropathol.* 2020;139:947-951.
57. Lynch DS, Jaunmuktane Z, Sheerin UM, et al. Hereditary leukoencephalopathy with axonal spheroids: A spectrum of phenotypes from CNS vasculitis to parkinsonism in an adult onset leukodystrophy series. *J Neurol Neurosurg Psychiatr.* 2016;87:512-519.
58. Konno T, Yoshida K, Mizuno T, et al. Clinical and genetic characterization of adult-onset leukoencephalopathy with axonal spheroids and pigmented glia associated with CSF1R mutation. *Eur J Neurol.* 2017;24:37-45.
59. Labauge P, Horzinski L, Ayrignac X, et al. Natural history of adult-onset eIF2B-related disorders: A multi-centric survey of 16 cases. *Brain.* 2009;132:2161-2169.